PHYSICAL REVIEW B, VOLUME 65, 134110

Molecular dynamics calculation of the ideal thermal conductivity of single-crystal α- and β-Si_3N_4

Naoto Hirosaki
Advanced Materials Laboratory, National Institute for Materials Science, 1-1 Namiki, Tsukuba-Shi Ibaraki 305-0044, Japan

Shigenobu Ogata
Department of Mechanical Engineering and Systems, Graduate School of Osaka University, 2-1 Yamada-oka, Suita-shi Osaka 565-0871, Japan

Cenk Kocer
Advanced Materials Laboratory, National Institute for Materials Science, 1-1 Namiki, Tsukuba-Shi Ibaraki 305-0044, Japan

Hiroshi Kitagawa and Yasuhiro Nakamura
Department of Adaptive Machine Systems, Graduate School of Osaka University, 2-1 Yamada-oka, Suita-shi Osaka 565-0871, Japan

(Received 24 September 2001; revised manuscript received 6 December 2001; published 22 March 2002)

The molecular dynamics method was used to simulate energy transport in α- and β-Si_3N_4 single crystals. The simulation data, in conjunction with the Green-Kubo formulation, was used to calculate the thermal conductivity of the single crystals, as a function of temperature. Although a relatively small simulation supercell size was employed, the thermal conductivity could be estimated with a reasonable degree of accuracy. In addition, simulated elastic constants of the crystals were found to be in reasonable agreement with existing data obtained from the literature. At a temperature of 300 K, it was estimated that the thermal conductivity (in units of $W\,m^{-1}\,K^{-1}$) in α- and β-Si_3N_4, along the *a* and *c* directions, is approximately 105 and 225, and 170 and 450, respectively. The results were compared to existing experimental data and, in particular, to the well-known Slack's equation. It was found that the current results are in reasonable agreement with existing results.

DOI: 10.1103/PhysRevB.65.134110 PACS number(s): 65.40.−b, 65.80.+n, 65.90.+i

I. INTRODUCTION

Silicon nitride (Si_3N_4) is currently a material of great research interest, because of its unique mechanical and electronic properties. In particular, it has been shown that silicon nitride exhibits excellent resistance to wear, corrosion, and thermal shock.[1] Furthermore, silicon nitride materials exhibit superior mechanical properties at elevated temperatures, and thus, it has been considered an ideal material for use in various applications, such as engine components, extrusion dies, and cutting tools.[1]

It is well known that there are two crystal structures of silicon nitride, α- and β-Si_3N_4, where the β configuration is the more stable of the two.[2] It is generally accepted that α and β are low- and high-temperature polymorphs, respectively, with a transformation of the α to β phase occurring at elevated temperatures above 1300 °C. Additionally, both of the configurations have an underlying atomic structure that is hexagonal and only differs along the *z* axis in the stacking sequence. Nevertheless, both of the configurations exhibit slightly different mechanical and thermal properties (for example, the α configuration is harder than the β configuration) that are not completely understood. Regardless of the difference between the two silicon nitride configurations, in order to understand, and thus control, the behavior of this type of ceramic at elevated temperatures some knowledge of the response of the material to temperature changes must be obtained.

Microstructure is important in understanding the thermal conductivity of a ceramic since the phases present, and the distribution of the phases, all have a significant effect on heat transport. In addition, porosity, grain boundaries, and structural defects (e.g., dislocations) are also important due to phonon, and photon, scattering. However, one factor that cannot be ignored is the effect of temperature on thermal conductivity. In general, increased temperatures result in increased lattice vibrations, which result in increased phonon scattering. In contrast, photon transport increases with temperature and may dominate in certain ceramics. In particular, in Si_3N_4 ceramics only acoustic phonons contribute significantly to heat transport. Although the magnitude of the thermal conductivity of most solids can be determined experimentally, it is desirable to have an estimate of the ideal thermal conductivity. Such an estimate can be used in the development of ''real'' materials. When the thermal conductivity of a ceramic is considered, along with the mechanical properties, suitable insight can be obtained, and microstructures can be developed to produce specific and desirable properties.

In this study, the ideal thermal conductivity of α- and β-Si_3N_4 single crystals was determined. Furthermore, the dependence of the thermal conductivity as a function of temperature was calculated. The calculations were performed using a molecular dynamics method, in conjunction with the Green-Kubo formulation. In the present paper, initially the simulation method will be outlined, including the procedure employed to calculate the thermal conductivity from the molecular dynamics data. Following this, the results of the simulation procedure will be presented, with a detailed discussion.

II. ESTIMATING THE THERMAL CONDUCTIVITY

Molecular dynamics is a numerical method that can be employed to estimate the characteristics of energy transport in a solid, due to lattice vibrations, at the atomic scale. Additionally, the molecular-dynamics method implicitly includes any anharmonic effects, which describe the vibrational mode couplings in an atomic lattice. These anharmonicities are essential for better characterizing the physical phenomena in solids, such as thermal conductivity. Therefore, molecular dynamics is one method that is well suited for the simulation of thermal conductivity in a solid. Clearly, however, it is appropriate to compare the molecular dynamics results to those of other existing methods. In the following sections the molecular dynamics procedure for estimating the thermal conductivity of α- and β-$\mathrm{Si_3N_4}$ single crystals, and various other methods, are outlined.

A. The molecular dynamics method

As mentioned, the molecular dynamics method can be used to study the characteristics of energy transport in a system. The molecular-dynamics technique, which in this case also incorporates the Green-Kubo method (discussed in the following section), has been employed successfully in the past to investigate the thermal properties of silicon crystals,[3] KCl,[4] and diamond.[5] In the case of $\mathrm{Si_3N_4}$, lattice vibrations are assumed to govern energy transport, which are modeled on predefined potential functions. The total potential energy, for $\mathrm{Si_3N_4}$ structures, of the system (E_T) was defined as the sum of two- $[E_{ij}^{(2)}(r_{ij})]$ and three-body $[E_{jik}^{(3)}(r_{ij},r_{ik},\theta_{jik})]$ interactions as proposed by Vashishta *et al.*,[6]

$$E_T=\sum_{i<j} E_{ij}^{(2)}(r_{ij})+\sum_{i,j<k} E_{jik}^{(3)}(r_{ij},r_{ik},\theta_{jik}), \qquad (1)$$

where *i*, *j*, and *k* refer to atoms in the system, r_{ij} is the length of the *ij* bond, and θ_{jik} is the bond angle between the *ij* and *ik* bonds. The two- and three-body energy terms are given as

$$\begin{aligned}E_{ij}^{(2)}(r_{ij})={}&A_{ij}\left(\frac{\sigma_i+\sigma_j}{r_{ij}}\right)^{\eta_{ij}}+\frac{Z_iZ_j}{r_{ij}}e^{(r_{ij}/r_{s1})}\\&-\frac{\alpha_iZ_j^2+\alpha_jZ_i^2}{2r_{ij}^4}e^{(r_{ij}/r_{s4})}, \qquad (2)\end{aligned}$$

$$\begin{aligned}E_{jik}^{(3)}(r_{ij},r_{ik},\theta_{jik})={}&B_{jik}e^{[(l/r_{ij}-r_c)+(l/r_{ij}-r_c)]}\\&\times[\cos\theta_{jik}-\cos\theta_{jik}^0], \qquad (3)\end{aligned}$$

where A, σ, η, Z, r_{s1}, α, r_{s4}, B, l, r_c, and θ^0 are parameters, determined for $\mathrm{Si_3N_4}$ by Vashishta *et al.*[6]

The two-body potential function consists of steric repulsion, Coulomb interaction, and dipole interaction through electronic polarization. The three-body function involves bond-bending terms, to take into account covalent bonding. This latter potential has been applied to various molecular dynamics calculations and has resulted in excellent predictions of equilibrium lattice parameters, elastic constants, phonon densities of states, and specific-heat data.[6–9]

It has been shown that it is important to take into account quantum corrections for low-temperature molecular dynamics simulations of the thermal conductivity.[10] The quantum correction is necessary in order to include the quantum occupation of phonon states, which differs significantly from the classical Boltzmann distribution. In general, this is accomplished by rescaling the temperature of the molecular-dynamics simulation.[10] Since the classical oscillator in a molecular dynamics system is different from that of a quantum oscillator, the mean kinetic energy of the molecular-dynamics system should be equal to the quantum system at low temperatures. Nevertheless, this effect is only significant for temperatures below approximately 300 K.[10] In this study, the thermal conductivity is only calculated for temperatures equal to or greater than 300 K and thus quantum corrections are not used.

B. The Green-Kubo method

Although the molecular dynamics method can be used to characterize energy transport, no direct information of the thermal conductivity can be obtained. Instead, the thermal conductivity κ is calculated using the Green-Kubo[11] method, which is based on the evaluation of the decay of equilibrium fluctuations of the heat flux vector $S(t)$ of the simulated system. The heat flux vector[12] for a system of atoms is defined as

$$S(t)=\frac{d}{dt}\sum_i r_i\tilde{E}_i=\sum_i \nu_i\tilde{E}_i+\sum_{i,j,i\neq j}(F_{ij}\cdot\nu_i)r_{ij}, \qquad (4)$$

where ν_i is the velocity of atom *i*, F_{ij} and r_{ij} represent the force acting on atom *i* due to atom *j* and the directional vector from atom *i* to atom *j* (where $r_{ij}=r_i-r_j$), respectively, and $\tilde{E}_i$ is the excess amount of site energy at atom *i*. In Eq. (4) the first term, $\Sigma_i\nu_i\tilde{E}_i$, is a convection term that describes atomic diffusion, and contributes significantly only at high temperatures. The second term, $\Sigma_{i,j,i\neq j}(F_{ij}\cdot\nu_i)r_{ij}$, represents the correlation between neighboring atoms and includes anharmonic effects.[10] All of the quantities in Eq. (4) can be determined directly from the molecular-dynamics simulation results. Additionally, $\tilde{E}_i$ can be obtained from the following relation (the sum of the two- and three-body terms of the potential and kinematic energy),

$$\tilde{E}_i=\sum_{\substack{j\\ i\neq j}} E_{ij}^{(2)}(r_{ij})+\sum_{\substack{jk\\ i\neq j,i\neq k,j>k}} E_{jik}^{(3)}(r_{ij},r_{ik},\theta_{jik})+\tfrac{1}{2}m_i|\nu|_i^2, \qquad (5)$$

where $E_{ij}^{(2)}$ and $E_{jik}^{(3)}$ are defined in Eqs. (2) and (3), respectively, and m_i is the mass of atom *i*. Thus, the directional thermal conductivity can be related directly to the time correlation function of the heat flux vector using the relation

$$\kappa_x(T)=\frac{1}{k_B V T^2}\int_0^\infty \langle S_x(0)S_x(t)\rangle dt, \tag{6}$$

where S_x is the heat flux vector along the x direction (and the relation is the same in the y and z directions), V the volume of the system, T the temperature of the system, and k_B is Boltzmann's constant.[10] There are several methods for evaluating the Green-Kubo[11] expression, which is directly related to estimating the time correlation function, using the data obtained from the molecular dynamics procedure. In this study, both direct and indirect methods are employed to estimate the time correlation function in Eq. (6).

In this study, the direct method of estimating the time correlation function of the heat flux vector was performed using a *double averaging method*. The ensemble, represented by the heat flux vector, was divided into subensembles for a given initial value. For example, in the case of the thermal conductivity in the x direction [given by Eq. (6)], $S_x(0)=S_x(\tau_o)$, and a final value $S_x(\tau_o+\tau)$, which represents many microscopic states with a given macroscopic value, $S_x(0)$. The time average of each individual subensembles was calculated, and then the average over all subensembles was determined, to obtain the time correlation function. Using the time average of the subensemble, in a discretized form, the non-normalized correlation function in the x direction can be written as

$$\langle S_x(0)S_x(t)\rangle=\frac{1}{\tau_{\max}}\sum_{\tau_o=1}^{\tau_{\max}} S_x(\tau_o)S_x(\tau_o+\tau), \tag{7}$$

where the average is over $\tau_{\max}$ time origins, which is the total number of subensembles. Clearly, in this case, for each value of τ_o, the value of $\tau_o+\tau$ must not exceed the maximum simulation time. More importantly, if the time step τ were too large the statistics of this long time would be poor, since there would exist few terms in the summation of Eq. (7). In general, the time correlation function should decay to zero in a time that is short compared to the total simulation time, and thus only a short time (equivalent to a few hundred data points) is of interest. Furthermore, for a short time τ, the correlation function can be determined with greater statistical accuracy because the total number of subensembles in the average would be greater. The time origin of each subensemble should not be defined such that they are successive data points, even though this is suggested in the definition of Eq. (7). Instead, the summation should be determined for time origins that are sufficiently distant in time. This is the case since successive origins in time would be highly correlated.

In general, the direct method of calculating the correlation function may require a large number of data points and lead to difficulties, since the time correlation of the heat flux vector decays very slowly with time. This can be avoided by using an indirect method, which is based on the Fourier transform of the thermal conductivity, defined by the expression[3,10]

$$\kappa(\omega,T)=\frac{1}{k_B V T^2}\int_{-\infty}^{\infty} \langle S_x(0)S_x(t)\rangle e^{i\omega t} dt, \tag{8}$$

where ω is the frequency, and S_x is the heat flux vector along the x direction. It is then easy to show that the thermal conductivity can be defined as the zero-frequency limit of Eq. (8).[10] The indirect Fourier-transform method can be validated by comparing the zero-frequency extrapolation with the time integral of the thermal conductivity, given in Eq. (6). It has been shown, previously, that the Fourier-transform analysis is consistent with the time-integral result.[10]

C. Slack's equation: An analytical approach

In 1954, Liebfried and Schlömann[13] reported an analytical treatment of the lattice vibrations in a face-centered-cubic crystal structure, which consisted of only one atom type per unit cell (i.e., a rare-gas crystal). This treatment was used to analytically determine the thermal conductivity of the crystal, above the Debye temperature. The treatment was improved by Julian,[14] to correct an intrinsic counting error, and then generalized by Slack,[15] to make it suitable for complex crystal structures. The derivation of Slack's equation is beyond the scope of this study. Nevertheless, the relevant equations will be presented and the calculated results compared to the molecular dynamics (MD) results.

Slack's equation assumes that heat transport in the crystal is dominated by acoustic vibrations, the dominant scattering mechanism is phonon-phonon scattering, and it is only valid at temperatures equal to or higher than the Debye temperature. Slack's equation for the maximum achievable thermal conductivity in nonmetallic solids, with complex crystal structures, can be written as[16]

$$\kappa=\frac{B\overline{M}\delta\theta^3}{\gamma^2 n^{2/3} T} \quad \text{for } T\geqslant\theta, \tag{9}$$

where B (in $\mathrm{W\,mol\,kg^{-1}\,m^{-2}\,K^{-3}}$) is a constant (which is dependent on γ),[15,16] $\overline{M}$ ($\mathrm{kg\,mol^{-1}}$) is the mean atomic mass, δ^3 ($\mathrm{m^3}$) is the average unit-cell volume, θ (K) is the acoustic-mode Debye temperature at absolute zero as calculated from elastic constants,[15] γ (dimensionless) is the Grüneisen parameter, n (dimensionless) is the number of atoms per unit cell, and T (K) is the absolute temperature.

Recently, it has been shown that the accuracy of Slack's equation can be improved considerably.[16] This is the case because the thermal-conductivity result is highly sensitive to the input parameters, in particular, the Debye temperature and Grüneisen parameter. It has been estimated that an error in the Debye temperature of ~10% can result in an error as high as 40% in the thermal conductivity. Additionally, a similar error of ~10% in the Grüneisen parameter can result in an error as high as 20% in the thermal conductivity. In particular, it has been shown that Slack's equation, with some modifications, can be applied to temperatures below the Debye temperature.[16]

As mentioned, the general Slack's equation is only valid in the region where the temperature is equal to or higher than the Debye temperature. In general, it is common practice to extrapolate data from this region to room temperature, 300 K. However, Bruls[16] has shown that a modified Slack's equa-

TABLE I. A list of the Slack's equation parameters and the corresponding values for the α- and β-Si_3N_4 single crystals.

Slack's equation parameters	α-Si_3N_4	β-Si_3N_4
$B(\gamma)$	$3.15e^7$	$3.15e^7$
$\bar{M}$	0.02	0.02
δ	$2.18e^{-10}$	$2.18e^{-10}$
γ	0.61	0.61
n	28	14
θ_h	1200	1200
θ_m	837	837
b	2	2

tion can be formulated to determine, with greater accuracy, the thermal conductivity below the Debye temperature. This equation can be written

$$\kappa=\frac{B\bar{M}\delta[\theta_m]^2}{\gamma^2 n^{2/3}}\left[\left(\frac{F_D\left(\frac{\theta_h}{T}\right)}{3R}\right)[(e^{\theta_h/(bTn^{1/3})})-1]bn^{1/3}\right], \tag{10}$$

where $F_D(\theta_h/T)$ is the Debye function,[16,17] θ_h is the high-temperature limit of the Debye temperature, θ_m is the minimum Debye temperature, R is the gas constant 8.314 ($\mathrm{J\,mol^{-1}\,K^{-1}}$), and b is a constant (where $b\cong 2$ for most solids[18]). It is trivial to show that Eq. (10) simplifies to the original Slack's equation, Eq. (9), for the limit $T \gg \theta_h$.

In this study, for evaluating Slack's equation, the input parameters of greatest importance are θ_h, the high-temperature limit of the Debye temperature, θ_m, the minimum Debye temperature, and γ, the Grüneisen parameter. It is assumed that only the acoustic phonons contribute to heat transport, in particular, at low temperatures. Therefore, the Debye temperature and the Grüneisen parameter should be derived from the acoustic vibration modes only.[15,19] Furthermore, the Debye temperature (for silicon nitride) as a function of temperature shows a minimum at approximately 50 K.[20] Since the low-temperature behavior is governed by acoustic vibration modes, this minimum value is suggested as a better estimate for the high-temperature limit related to acoustic phonons. It is also suggested that the Grüneisen parameter should be defined over all temperatures as the thermodynamic Grüneisen parameter evaluated at the minimum Debye temperature, which describes better the acoustic-mode vibrations. The values adopted for the Slack's equation parameters are listed in Table I, and were collected from the literature.[15,16,19,20]

D. An estimate of the thermal conductivity of isotropic polycrystalline silicon nitride

Currently, few experimental measurements of the thermal conductivity of silicon nitride single crystals have been reported. This is due, in part, to the difficulty associated with growing single crystals of silicon nitride ceramics. Nevertheless, the current simulation results can be used to estimate the thermal conductivity of isotropic polycrystalline silicon nitride, for which some data have been reported in the literature. In the case of macroscopically isotropic polycrystals, certain material properties, such as the thermal properties (for obvious reasons in this study only the thermal conductivity is considered), can be estimated from the properties determined in the corresponding anisotropic single-crystal material. The most well-known formulations for such estimates are the expressions for the arithmetic (AM) and harmonic (HM) means of the thermal conductivity,[21,22]

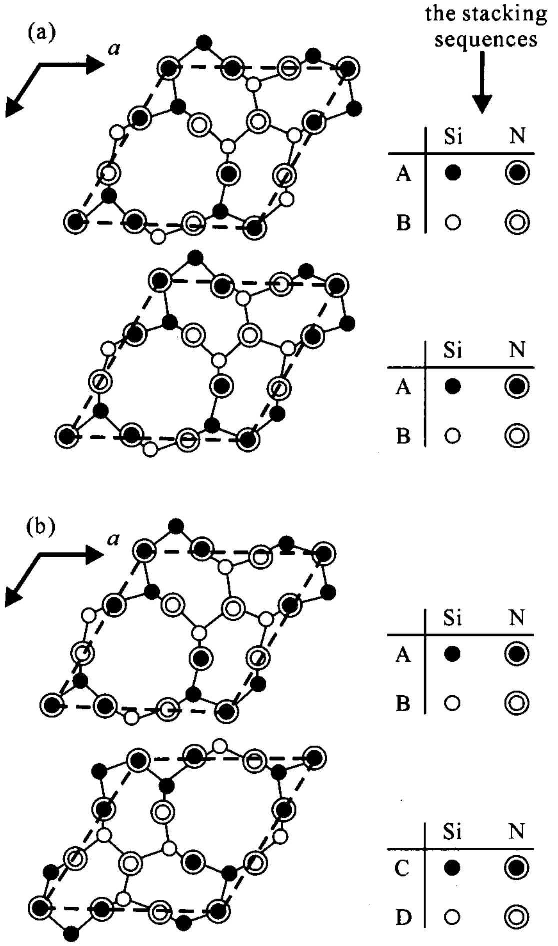

FIG. 1. Crystal structure of the (a) α- and (b) β-Si_3N_4 single crystals, in which the Si-N layers are stacked as AB···AB and ABCD···ABCD, respectively.

$$\kappa_{\mathrm{AM}}=\tfrac{1}{3}(\kappa_1+\kappa_2+\kappa_3), \tag{11}$$

$$\frac{1}{\kappa_{\mathrm{HM}}}=\tfrac{1}{3}\left(\frac{1}{\kappa_1}+\frac{1}{\kappa_2}+\frac{1}{\kappa_3}\right), \tag{12}$$

where κ_{AM}, κ_{HM} are estimates of the isotropic polycrystalline thermal conductivity, and κ_i $\{i=1, 2, 3\}$ represents the anisotropic crystalline thermal conductivity in the x, y, and z directions, respectively. It should be noted that these two solutions are a lower, Eq. (12), and upper, Eq. (11), bound of the estimate for the polycrystalline structure[21] (they are known as the elementary bounds). However, there has been

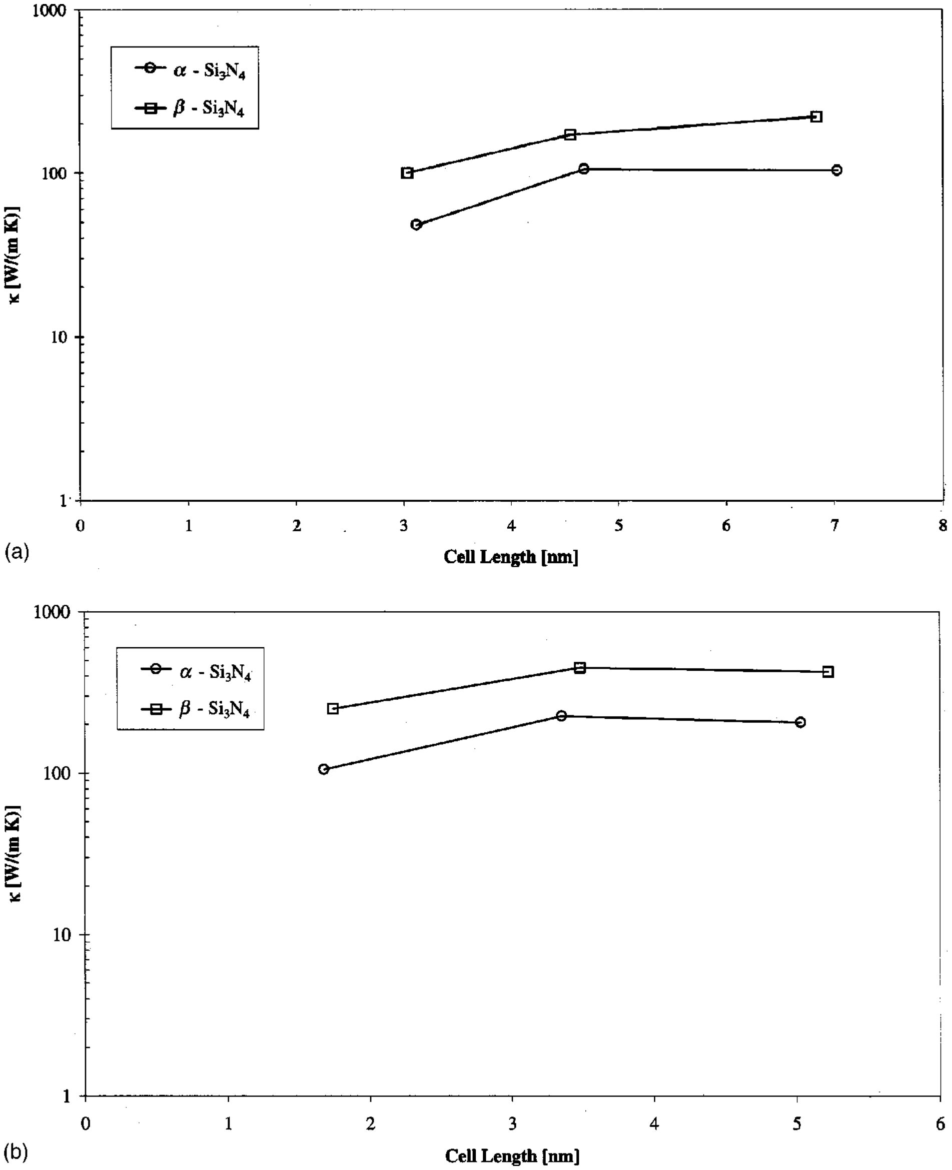

FIG. 2. Plot of thermal conductivity (at a constant temperature of 300 K) as a function of the supercell characteristic length in the (a) *a*- and (b) *c*-axial directions.

some discussion in the past as to the applicability of this result. Various authors have reported formulations based on variational principles,[23–25] which lead to narrower bounds. Recently, however, Adams and Olson[21] have shown that although tighter bounds could be obtained using the variational principle methods, the results were based on questionable assumptions. Thus, in this study, the *classical* elementary bounds [Eqs. (11) and (12)] calculated from the simulation data of the single crystals are used to estimate a range for the thermal conductivity of isotropic polycrystalline silicon nitride. It is important to note that the range calculated is a rough estimate, which does not include the effect that structural anomalies, such as grain boundaries, would have on the thermal conductivity of the material.

III. MOLECULAR DYNAMICS SIMULATION RESULTS

The crystal structure of both α- and β-$\mathrm{Si_3N_4}$ can be considered to contain the fundamental Si-$\mathrm{N_4}$ tetrahedra structure, joined together by shared corners in a three-dimensional network. The structures consist of layers of silicon and nitrogen in a sequence, along the *c* axis, as illustrated in Figs. 1(a) and 1(b). The α- and β-$\mathrm{Si_3N_4}$ structures both exhibit hexagonal symmetry represented by the space groups $P31c$ and $P6_3$, respectively.[2] The relevant elastic constants for the two silicon nitride phases[26] are C_{11}, C_{33}, C_{44}, C_{66}, C_{12}, and C_{13}, where C_{22} is equivalent to C_{11}, C_{55} is equivalent to C_{44}, and C_{66} is calculated using the relation $C_{66}=\frac{1}{2}(C_{11}-C_{12})$.

The elastic constants of the α- and β-$\mathrm{Si_3N_4}$ single crystals can be calculated using the total potential-energy term given by Eq. (1). The tensors of the elastic constants C_{ij} are expressed using the total potential energy E_T,[27]

$$C_{ij}=\frac{1}{V}\frac{\partial^2 E_T}{\partial\varepsilon_i\partial\varepsilon_j}, \tag{13}$$

where $i,j=1$, 2, 3, 4, 5 and 6, and is equivalent to the components *xx*, *yy*, *zz*, *yz*, *zx*, and *xy*, respectively, ε_i and ε_j are small strains, and V is the volume of the model. For the

TABLE II. Relevant structural data for the α- and β-Si_3N_4 single-crystal supercells, used in the molecular dynamics simulation procedure.

α-Si_3N_4	
Number of atoms	672
Optimum supercell dimensions (nm)	a direction: $x=4.7$, $y=1.4$, $z=1.7$ c direction: $x=1.6$, $y=1.4$, $z=3.4$
Lattice Constants (nm)	$a=0.7818$, $c=0.5591$
β-Si_3N_4	
Number of atoms	672
Optimum supercell dimensions (nm)	a direction: $x=4.6$, $y=1.3$, $z=1.7$ c direction: $x=1.7$, $y=1.3$, $z=3.5$
Lattice constants (nm)	$a=0.7595$, $c=0.2902$

elastic constant calculations, all simulations were for canonical, NVT ensembles at 300 K. It should be noted that the calculations were performed at 300 K, since the lattice parameters for the material structure were obtained experimentally at this temperature.[2,28] Equation (13) suggests that the elastic constants can be calculated by differentiating the interatomic potential with respect to strain. Thus, the MD unit cell was deformed prior to the MD procedure by a predefined amount of ε_i and ε_j (approximately 10^{-3} in magnitude), and E_T was calculated using Eq. (1) by finding the minimum-energy point. The C_{ij} values were calculated by numerically differentiating E_T in Eq. (13) by ε_{ij} and ε_{kl}, at the minimum-energy point. It should be noted that in Eq. (13) the kinetic-energy term of the system was not included. In general, the kinetic term is negligible and, thus, was not included so as to simplify the calculation.[27,28]

The supercell dimension, in the direction of the heat flux calculation, has a significant effect on the accuracy of the estimated thermal conductivity and on the computation time. It was necessary, therefore, to estimate an optimum supercell size. The thermal conductivity was calculated for various supercell lengths in the a and c directions, at a constant temperature of 300 K, presented in Figs. 2(a) and 2(b), respectively. It is clear from the data that the optimum characteristic length in the a direction is ~4.7 nm and in the c direction is ~3.5 nm.

Thus, the unit cell of the α-Si_3N_4 single crystal for the simulation contained 12 silicon and 14 nitrogen atoms. Correspondingly, the β-Si_3N_4 single-crystal unit cell contained six silicon and eight nitrogen atoms. The typical supercell employed in this study contained 672 atoms, constructed from a predefined number of unit cells. The relevant structural data of the α- and β-Si_3N_4 single-crystal supercells are summarized in Table II. Periodic boundary conditions were imposed along each direction of the supercell, to ensure energy (and momentum) conservation while allowing energy to flow through the boundaries.

Initially, for a predefined temperature, constant volume, and constant number of atoms, the atomic configuration (of the supercell) was relaxed to equilibrium (a force-free mechanically stable configuration) over a period of approximately 12 ps. After equilibration, the molecular dynamics simulation was carried out for approximately 3.5 ns, during which the heat flux vector S was calculated (at constant volume, constant total system energy, and constant number of atoms) approximately every 1.2 fs.

As mentioned previously, there exists direct and indirect methods of calculating the temperature-dependent thermal conductivity from the molecular-dynamics simulation results. In this study, the thermal conductivity was calculated using both methods. In the case of the direct method, a double averaging method, the thermal conductivity was calculated for an averaging time of approximately 12 ps. This averaging time, over the total simulation time of 3000 ps, is equivalent to approximately 250 subensembles. The thermal conductivity was then calculated by averaging the subensemble results, over all subensembles. The thermal-conductivity result as a function of the averaging time is presented in Fig. 3. It is clear from the results that a short averaging time leads to inaccurate results. Furthermore, it should be clear that a long averaging time would also lead to inaccurate results, as mentioned in Sec. II.

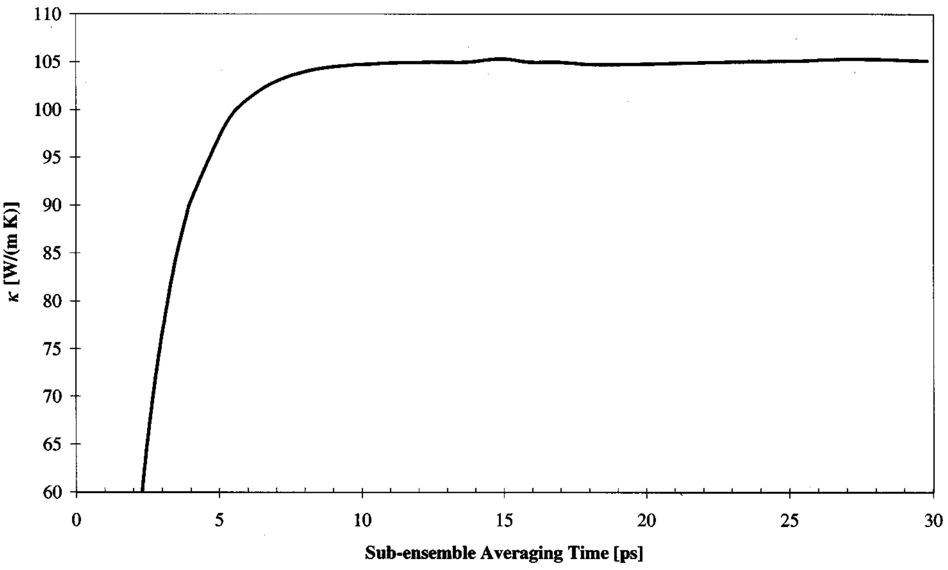

FIG. 3. A typical plot of thermal conductivity, as a function of the subensemble averaging time, obtained using the double averaging method. This data is for α-Si_3N_4 at 300 K in the a-axis direction.

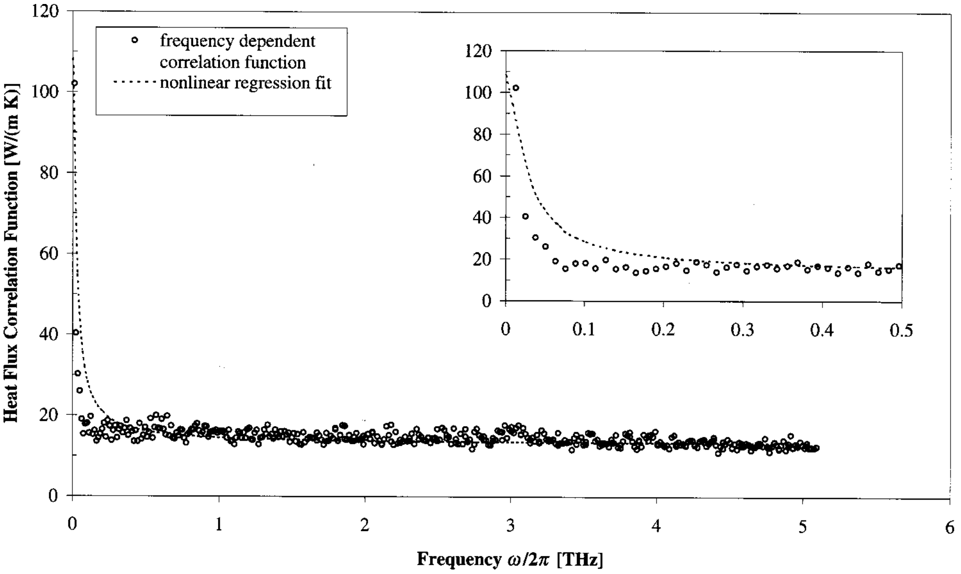

FIG. 4. A typical plot of the frequency-dependent heat flux correlation function, as a function of frequency (circles), and nonlinear fitting result (dashed lines). This data is for α-Si_3N_4 at 300 K in the a-axis direction. The inset shows the same data in the short-time region.

The indirect method, a Fourier-transform analysis, was calculated for the zero-frequency limit. A typical plot of the frequency-dependent heat flux correlation function is presented in Fig. 4. A fit of the data, using a nonlinear least-squares method,[5] was applied to determine the zero-frequency limit. To fit the correlation function a double exponential function was employed,[5]

$$\langle S_x(0)S_x(t)\rangle = A_o e^{(-t/\tau_o)} + A_a e^{(-t/\tau_a)}, \tag{14}$$

where the subscripts o and a denote optical and acoustic modes, respectively. After a simple substitution [into Eq. (8)], and integration, it is found that the frequency-dependent thermal conductivity is given by the following equation,

$$\kappa(\omega,T) = \frac{1}{k_B V T^2}\left[\left(\frac{A_o}{\sqrt{(\omega^2+\tau_o^{-2})}}\right) + \left(\frac{A_a}{\sqrt{(\omega^2+\tau_a^{-2})}}\right)\right], \tag{15}$$

where, as mentioned previously, the static thermal conductivity is obtained from the zero-frequency limit $\kappa(0,T)$. It is important to note that the nonlinear fitting result, Fig. 4, diverges from the simulation result for low frequencies (<2 THz). It is understood that the behavior in this region is related to an overestimation in the correlation function for low frequencies.[3] The periodic boundary conditions induce correlation artifacts in the correlation function. Thus, the higher-frequency data are more favorable, and in this case the fitting at higher frequencies is more reliable. The typical results of the direct and indirect methods, in the direction of the a axis, for α-Si_3N_4, are presented in Fig. 5 for comparison. It is clear that the data from both methods agree well. It was found that typically the optical modes have a relaxation time on the order of $\sim 3.68e^{-5}$ ps and the acoustic modes are on the order of $\sim$9.5 ps. In addition, the optical modes are found to contribute a maximum of $\sim$8% to the thermal conductivity.

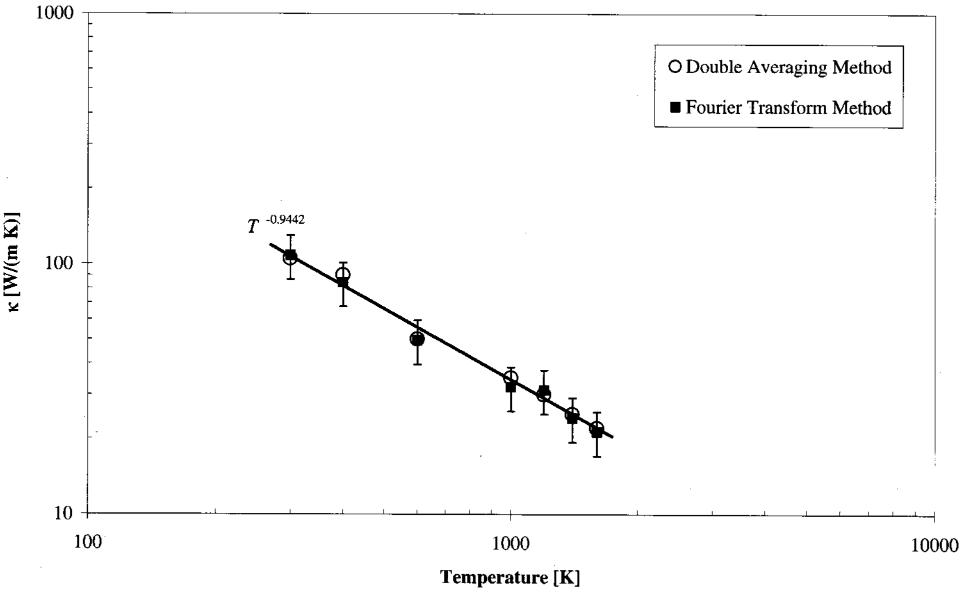

FIG. 5. A typical plot of the thermal conductivity as a function of temperature, as determined from the double averaging and Fourier-transform methods. This data is for α-Si_3N_4 in the a-axis direction.

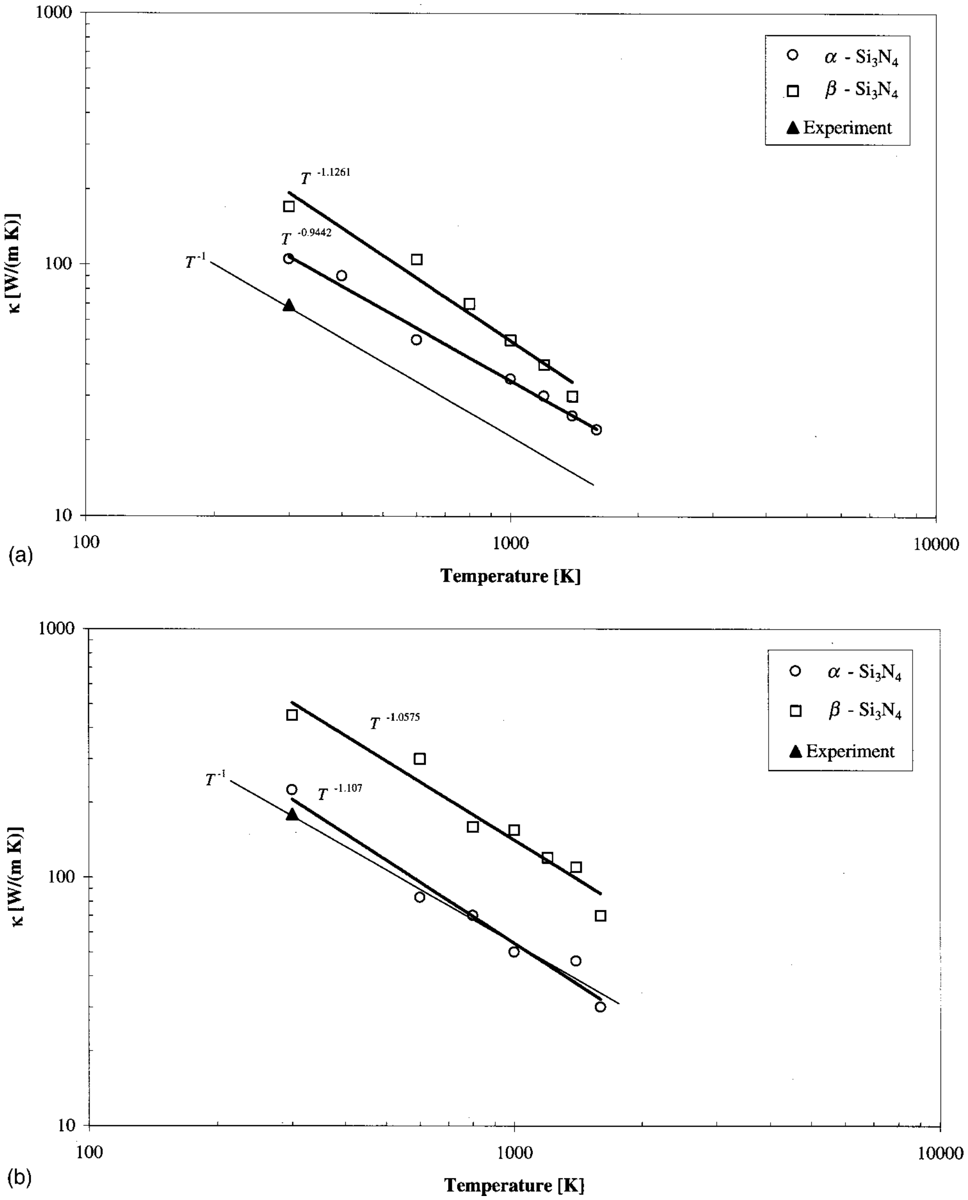

FIG. 6. Plot of the thermal conductivity as a function of temperature, for the α- and β-Si_3N_4 single crystals, in the (a) *a*- and (b) *c*-axial directions.

The data of the thermal conductivity, for the α- and β-Si_3N_4 single crystals, as a function of temperature, in the *a* and *c* directions are presented in Figs. 6(a) and 6(b), respectively. It is important to note that an arbitrary choice was made and the data given in Figs. 6(a) and 6(b) are the results obtained from the direct, double averaging, method. The molecular dynamics results are also compared against results obtained from other sources, such as Slack's equation and experimental measurements reported in the literature,[15,21,29–31] in Table III for 300 and 1400 K. The elastic constants for the α- and β-Si_3N_4 single crystals were also estimated, and are presented in Table IV along with data reported in the literature.[26,32–34]

IV. DISCUSSION

The material elastic constants calculated using the current numerical procedure are presented in Table IV. Numerous theoretical[26,32] and experimental[33,34] studies have reported elastic constants for silicon nitride ceramics. From the data presented in this study, the theoretical results are from Wendal and Goddard III,[26] and Ching *et al.*,[32] where the elastic constants were derived from an *ab initio* force field molecular-dynamics simulation and an *ab initio* total-energy calculation, respectively. Correspondingly, the experimental measurements are from Vogelgesang and Grimsditch,[33] and Hay *et al.*,[34] determined using Brillouin scattering and nanoindentation measurements, respectively. However, the reported data are limited to β-Si_3N_4. Regardless, the data in Table IV indicate that the simulation results are in reasonable agreement with existing data found in the literature.

In this study, the phonon mean free path in the crystals examined can be on the order of tens of nanometers. Thus, it is reasonable to expect that for accurate results the characteristic supercell dimension should be as large, if not larger, than the phonon mean free path. The phonon mean free path, of the silicon nitride systems, can be calculated using the

TABLE III. A comparison of the current molecular dynamics results, and the existing results found in the literature for various methods.

	α-Si_3N_4				β-Si_3N_4			
	300 K		1400 K		300 K		1400 K	
Anisotropic single-crystal results	*a* axis	*c* axis	*a* axis	*c* axis	*a* axis	*c* axis	*a* axis	*c* axis
MD simulation	105	225	25	46	170	450	30	110
Single-crystal experimental results[a]					69	180		
Isotropic polycrystalline results								
Slack's equation[b]	115.20–46.90		16.87		249.71–77.30		26.77	
Elementary bounds from MD results[c]	128.0–145.0		29.5–32.0		214.5–263.0		39.6–56.7	
CVD[d] and sintered[e] specimen experimental results	~59.0		~19.7		~122.0		~28.0	

[a] Reference 27.
[b] Reference 15.
[c] Reference 21.
[d] Reference 28.
[e] Reference 26.

thermal-conductivity equation obtained from the kinetic theory of gases,[35]

$$\kappa = \tfrac{1}{3}\nu_p C\langle l_p\rangle, \qquad (16)$$

where ν_p is the phonon velocity, C is the heat capacity, and $\langle l_p\rangle$ is the phonon mean free path. Using the simulated elastic constants to estimate the phonon velocity, the simulated thermal conductivity, and the experimentally determined heat capacity, the phonon mean free path was calculated for a temperature of 300 K. The estimated results are presented in Table V. Clearly, the shortest mean free path is approximately 14 nm, which is much larger than the smaller optimum supercell size of approximately 3.5 nm, estimated from Fig. 2. When the supercell size is small, there is the possibility of a periodically equivalent phonon traveling through the supercell, and returning to the phonon point of origin. However, it is possible to obtain accurate thermal-conductivity results for a characteristic supercell dimension much smaller than the phonon mean free path.[5] This is the case since in the method employed in this study the energy current correlation time is much shorter than the energy relaxation time. A rigorous proof is not given here as a matter of convenience, however, Che *et al.*,[5] and Volz and Chen[3] provide a detailed analysis of the current correlation function method.

TABLE IV. Elastic constants calculated using the current molecular dynamics procedure, for the α- and β-Si_3N_4 single crystals.

	α-Si_3N_4	β-Si_3N_4		
	This work (GPa)	This work (GPa)	Theoretical results[a,b] (GPa)	Experimental results[c,d] (GPa)
C_{11}	593	591	315–591	343–433
C_{33}	579	690	332–690	574–600
C_{44}	174	189	108–114	108–124
C_{66}	207	205	69–134	~119
C_{12}	179	182	181–271	136–195
C_{13}	165	162	150–200	120–127

[a] Reference 25.
[b] Reference 29.
[c] Reference 30.
[d] Reference 31.

TABLE V. An estimate of the phonon velocity and phonon mean free path, as determined from the elastic constants calculated using the molecular dynamics procedure. The data were calculated for a temperature of 300 K. It should be noted that in the case of the phonon mean free path, the current thermal conductivity, the experimentally determined heat capacity, and the current phonon velocity were used in the calculation.

	α-Si_3N_4		β-Si_3N_4	
Velocity components ($\times$) 10^4 ($m\,s^{-1}$)	*a* direction	*c* direction	*a* direction	*c* direction
ν_x	1.36	1.34	1.36	1.47
ν_y	1.04	1.04	1.09	1.09
ν_z	0.81	1.04	0.82	1.0
ν_{average}	0.98	1.11	0.99	1.17
Mean free path (nm)				
l_p	14	27	23	52

The thermal conductivity as a function of temperature, obtained from the molecular-dynamics procedure, is presented in Fig. 6. In addition to the simulation data presented in Fig. 6, the experimental measurement for a β-Si_3N_4 single crystal and a trend line of the T^{-1} behavior below 300 K are also shown. At present, to the best of our knowledge there are no reported experimental data of the thermal conductivity of a α-Si_3N_4 single crystal. In the case of the β-Si_3N_4 single crystal the lower experimental result was expected. The current results were calculated for a crystal structure with no impurities or structural defects. The ‘‘real’’ β-Si_3N_4 single crystal does contain structural anomalies and impurities and, thus, results in an increase in phonon scattering, resulting in a lower thermal conductivity.

In Fig. 6, the functional dependence of the simulated thermal conductivity to temperature is also shown. The dependence was estimated by calculating a power function of the best fit to the data. Clearly, within calculation error, the current data exhibits a behavior that is in good agreement with the T^{-1} behavior predicted by experimental data.[30] The T^{-1} behavior is also predicted by Eq. (16).[11] It is argued that, below the Debye temperature, the heat capacity C increases in proportion to T^3, approaching a constant value. In this temperature regime, the phonon velocity ν_p is not sensitive to temperature. However, the phonon mean free path $\langle l_p \rangle$ for temperatures above 300 K decreases as T^{-1} due to phonon-phonon scattering. It is well known that below 300 K, the mean free path is approximately constant since phonon scattering is dominated by temperature-independent phonon interactions at structural anomalies and surfaces.

In addition to Fig. 6, the simulation results at 300 and 1400 K are compared to other results, presented in Table III. In this table the results of Slack's equation, the elementary bounds (calculated from the molecular-dynamics data), and experimental measurements of silicon nitride are presented. Clearly, there exists far fewer reported data for α-Si_3N_4 (no theoretical or experimental data could be found in the literature) than for β-Si_3N_4. Furthermore, it should be clear that the experimental data presented are not expected to correlate well with the simulation results, because of structural differences. As mentioned previously, in the ‘‘real’’ silicon nitride ceramics, there are a large number of structural defects and numerous impurities, which result in an increase of phonon scattering. This is particularly the case with the α-Si_3N_4 experimental result because it was measured for a chemically vapor deposited (CVD) specimen,[31] which is a method that can result in various structural anomalies. However, considering the structural differences, the data presented in Table III are in relatively good agreement.

The Slack's equation results are of great interest, since the Slack's equation was derived for a defect-free crystalline solid, where phonon-phonon interactions are presumed to be the main source of phonon scattering. However, in Eq. (10) for the temperature regime below the Debye temperature the value $b \cong 2$, assumed for most solids, is questionable. Hence, the values of the Slack's equation for 300 K are presented for a range of values, $b \cong 0.5$ to 3, where the lower b values result in a higher thermal conductivity. The resulting range of values suggests that the thermal conductivity is sensitive to the value chosen for the material constant b. In particular, a value $b < 1$ may be more representative of the silicon nitride ceramics.

The simulation results are in reasonable agreement with Slack's equation, where better agreement is obtained for the β-Si_3N_4 single crystal. This maybe the case since the β-Si_3N_4 single crystal has only half as many atoms per unit cell. In Slack's equations $\kappa \sim n^{-2/3}$, however, $\kappa \sim n^{-1/3}$ and $\kappa \sim n^{-1/2}$ have also been reported in the literature.[36] From the simulation results it is found that $\kappa \sim n^{-1 \pm 0.5}$. The dependence of the thermal conductivity on the number of atoms per unit cell is a point of contention that requires further investigation. However, it has been shown by an extensive study[37] that, although the tetrahedral atomic structure is favorable for a high thermal conductivity, a higher coordination number does result in a lower thermal conductivity. It is important to note that in general, however, the Slack's equations are based on assumptions, which limit the accuracy of the results. The assumptions clearly neglect the possibility of heat transport by photons, charge carriers, polarons, etc. and also neglect other possible scattering processes, such as impurities, vacancies, dislocations, grain boundaries, crystal boundaries, etc.[15] In addition, as mentioned previously, the values of several of the parameters in Slack's equation are difficult to define. For example, in Eq. (10) by using the thermodynamic Grüneisen parameter for γ, there is no distinction made between the acoustic and optic phonons.[16]

It is clear from the main results of this study that the silicon nitride ceramics are a class of materials with excellent thermal conductivity. This is particularly the case with the β-Si_3N_4 single crystal. However, the current investigation has not attempted to determine the effects of impurities and structural defects on the thermal conductivity. In order to ascertain such effects, it is suggested that the molecular-dynamics calculation be employed to investigate atomic configurations that have such anomalies introduced into the crystal structure. The ability to introduce specific atomic impurities at specific atomic lattice locations, also the case when looking at the effect of structural defects, would be of significant advantage. It is already well known that such anomalies significantly affect thermal properties of a solid. It is the intention of the current authors to investigate such effects using the molecular-dynamics procedure. It is expected that such a study would result in a greater understanding of the mechanisms of heat transport in solids.

V. CONCLUSION

In this study, the molecular dynamics method was used to simulate energy transport in α- and β-Si_3N_4 single crystals. Using the simulation data, the Green-Kubo formulation was applied to calculate the thermal conductivity of the single crystals, as a function of temperature. It was found that the thermal conductivity could be estimated with a high degree of accuracy, even though a relatively small simulation supercell size was employed. The calculated elastic constants of the crystals were found to be in reasonable agreement with existing data obtained from the literature. At a temperature of 300 K, it was determined that the thermal conductivity (in units of $\mathrm{W\,m^{-1}\,K^{-1}}$) in α-Si_3N_4 and β-Si_3N_4, along the a and c directions, is approximately 105 and 225, and 170 and 450, respectively. It is clear from comparisons with existing experimental data that a higher thermal conductivity for silicon nitride could be obtained, if the existing methods for producing the ceramics could be refined to result in fewer structural defects and impurities. This is particularly the case with the β-Si_3N_4 single crystal, which exhibits the higher thermal conductivity.

ACKNOWLEDGMENT

C.K. would like to acknowledge support from the Science and Technology Agency of Japan.

---

[1] F. de Brito Mota, J. F. Justo, and A. Fazzio, Phys. Rev. B **58**, 8323 (1998).

[2] R. Grün, Acta Crystallogr., Sect. B: Struct. Crystallogr. Cryst. Chem. **35**, 800 (1979).

[3] S. G. Volz and G. Chen, Phys. Rev. B **61**, 2651 (2000).

[4] G. V. Paolini, P. J. D. Lindan, and J. H. Harding, J. Chem. Phys. **106**, 3681 (1997).

[5] J. Che, T. Çağin, W. Deng, and W. A. Goddard III, J. Chem. Phys. **113**, 6888 (2000).

[6] R. Vashishta, R. K. Kalia, A. Nakano, and I. Ebbsjö, in *Amorphous Insulators and Semiconductors*, edited by M. F. Thorpe and M. I. Mitkova (Kluwer, Dortrecht, 1996), p. 151.

[7] C. K. Loong, P. Vashishta, R. K. Kalia, and I. Ebbsjö, Europhys. Lett. **31**, 201 (1995).

[8] A. Nakano, R. K. Kalia, and P. Vashishta, Phys. Rev. Lett. **75**, 3138 (1995).

[9] K. Tsuruta, A. Nakano, R. K. Kalia, and P. Vashishta, J. Am. Ceram. Soc. **81**, 433 (1998).

[10] Y. H. Lee, R. Biswas, C. M. Soukoulis, C. Z. Wang, C. T. Chan, and K. M. Ho, Phys. Rev. B **43**, 6573 (1991).

[11] H. Kitagawa, Y. Shibutani, and S. Ogata, Modell. Simul. Mater. Sci. Eng. **3**, 521 (1995).

[12] R. W. Zwanzig, Annu. Rev. Phys. Chem. **16**, 67 (1965).

[13] G. Leibfried and E. Schlömann, Nachr. Ges. Wiss. Goettingen, Math.-Phys. Kl. **2**, 71 (1954).

[14] C. L. Julian, Phys. Rev. **139**, A128 (1965).

[15] G. A. Slack, *Solid State Physics*, edited by F. Seitz, D. Turnbull, and H. Ehrenreich, (Academic, New York, 1979), Vol. 34, p. 1.

[16] R. J. Bruls, Ph.D. thesis, Technische Universiteit Eindhoven, 2000.

[17] C. Kittel, *Introduction to Solid State Physics*, 5th ed. (Wiley, New York, 1970), p. 178.

[18] J. R. Drabble and H. J. Goldsmid, *Thermal Conduction in Semiconductors, International Series of Monographs on Semiconductors*, edited by H. K. Henisch (Pergamon, London, 1961), Vol. 4, p. 141.

[19] C. Domb and L. Salter, Philos. Mag. **43**, 1083 (1952).

[20] R. J. Bruls, H. T. Hintzen, G. de With, R. Metselaar, and J. C. van Miltenburg, J. Phys. Chem. Solids **62**, 783 (2001).

[21] B. L. Adams and T. Olson, Prog. Mater. Sci. **43**, 1 (1998).

[22] S. Kumar and R. N. Singh, J. Am. Ceram. Soc. **78**, 728 (1995).

[23] Z. Hashin and S. Shtrikman, J. Mech. Phys. Solids **10**, 335 (1962).

[24] L. J. Walpole, J. Mech. Phys. Solids **14**, 151 (1966).

[25] M. W. Willemse and W. J. Caspers, J. Math. Phys. **20**, 1824 (1979).

[26] J. A. Wendal and W. A. Goddard III, J. Chem. Phys. **97**, 5048 (1992).

[27] Y. Shibutani, J. Soc. Mater. Sci. Jpn. **46**, 218 (1997).

[28] K. Kato, Z. Inoue, K. Kijima, J. Kawada, H. Tanaka, and T. Yamane, J. Am. Ceram. Soc. **58**, 90 (1975).

[29] N. Hirosaki, Y. Okamoto, M. Ando, F. Munakata, and Y. Akimune, J. Ceram. Soc. Jpn. **103**, 1345 (1996).

[30] K. Watari, J. Ceram. Soc. Jpn. **109**, S7 (2001).

[31] T. Hirai, S. Hayashi, and K. Niihara, Ceram. Bull. **57**, 1126 (1978).

[32] W-Y. Ching, Y-N. Xu, J. D. Gale, and M. Rühle, J. Am. Ceram. Soc. **81**, 3189 (1998).

[33] R. Vogelgesang and M. Grimsditch, Appl. Phys. Lett. **76**, 982 (2000).

[34] J. C. Hay, E. Y. Sun, G. M. Pharr, P. F. Becher, and K. B. Alexander, J. Am. Ceram. Soc. **81**, 2661 (1998).

[35] C. Kittle, *Introduction to Solid State Physics*, 5th ed. (Ref. 17), p. 186.

[36] M. Roufosse and P. G. Klemens, Phys. Rev. B **7**, 5379 (1973).

[37] D. P. Spitzer, J. Phys. Chem. Solids **31**, 19 (1970).